NIH Public Access
Author Manuscript
Semin Oncol. Author manuscript; available in PMC 2012 February 1.

Published in final edited form as:
Semin Oncol. 2011 February ; 38(1): 42–54. doi:10.1053/j.seminoncol.2010.11.002.

Molecular MR Contrast Agents for the Detection of Cancer: Past and Present

Alexei Bogdanov Jr and **Mary L. Mazzanti**
Department of Radiology, University of Massachusetts Medical School, Worcester MA

Abstract

Magnetic resonance imaging (MRI) is a powerful diagnostic tool capable of providing detailed information about the structure and composition of tumors, with unsurpassed spatial resolution. The use of exogenously administered contrast agents allows compartment-specific enhancement of tumors, enabling imaging of functional blood and interstitial volumes. Current efforts are directed at enhancing the capabilities of MRI in oncology to add contrast agents with molecular specificities to the growing armamentarium of diagnostic probes capable of changing local proton relaxation times as a consequence of specific contrast agent binding to cell surface receptors or extracellular matrix components. We review herein the most notable examples, illustrating major trends in the development of specific probes for high-resolution imaging in molecular oncology.

Introduction

Despite medical advances over the last decade, cancer persists as one of the most intractable of all human diseases. According to one report, the number of new cases of cancer will grow to almost 17 million by 2020, which translates into a one-third increased incidence of cancer over the current rate with an estimated global economic cost of 300 billion dollars [1]. The crisis has led the US Food and Drug Administration (FDA) and the National Cancer Institute (NCI) to sponsor major initiatives to bring new treatments, based on recent advances in molecular genomics, to the clinic. Although such strategies offer the hope of more targeted and personalized therapies, this will only translate into a reduction in morbidity and mortality if cancers can be diagnosed at an early stage, when the disease is still treatable.

Magnetic resonance imaging (MRI) is increasingly the imaging modality of choice for the detection and diagnosis of various benign and malignant tumors. Early on, the choice of MRI was based on the ability of this diagnostic modality to capture anatomical images at high (i.e., submillimeter) resolution without the radiation exposure associated with alternative cross-sectional tomographic techniques, such as positron emission and computed tomography (PET and CT). In MRI, contrast between tissues (and tumor compartments) is generated by differences in the relaxation rates of proton nuclear spins that exist across different tissues. Also of great utility in cancer detection is the ability of MRI to measure altered perfusion rates that result from the neovascularization of tumors. Although highly useful, MRI is still limited by its incapacity to detect malignancies in their earliest stages.

Corresponding author: Alexei Bogdanov, Jr, Ph.D., Professor of Radiology and Cell Biology, University of Massachusetts Medical School, S6-434, 55 Lake Ave North, Worcester MA 01655, Tel: (508) 856-5571, Fax: (508) 856-1860, Alexei.Bogdanov@umassmed.edu.

Publisher's Disclaimer: This is a PDF file of an unedited manuscript that has been accepted for publication. As a service to our customers we are providing this early version of the manuscript. The manuscript will undergo copyediting, typesetting, and review of the resulting proof before it is published in its final citable form. Please note that during the production process errors may be discovered which could affect the content, and all legal disclaimers that apply to the journal pertain.

NIH-PA Author Manuscript
NIH-PA Author Manuscript
NIH-PA Author Manuscript

NIH-PA Author Manuscript

NIH-PA Author Manuscript

NIH-PA Author Manuscript

Thus, a concerted effort has been made over the last decade to bring MRI into the realm of molecular imaging by using newly developed MR contrast agents for targeting cancer specific molecules and for recognizing cancer-specific microenvironments. Such agents, or imaging probes, should also prove useful in assessing new 'personalized' gene therapies, and in following patient long-term outcomes.

The most commonly used magnetic resonance (MR) techniques are based on detection of water proton resonances. The ultimate goal in the development of any disease-specific molecular MR contrast agent (CA) is to design a probe that, upon interacting with a cancer-specific target molecule *in vivo*, will create changes in local tissue proton relaxation times (spin-lattice, or longitudinal relaxation time, T_1, and spin-spin or transverse relaxation time, T_2) and thus generate changes in MR signal intensity in the vicinity of the targeted molecule. In addition, the CA should be easy to administer in a clinical setting and have an acceptable safety profile. To date, agents that fulfill these requirements have consisted of either chelated cations of the paramagnetic metal gadolinium (Gd^{3+}) or paramagnetic and super-paramagnetic iron oxide (IO) nanoparticles that are linked (either covalently or non-covalently) to disease-targeting molecules. Although seemingly straightforward, designing and producing Gd^{3+} or IO-based targeted MR CAs is challenging and even the compounds that reach the phase of *in vivo* testing are often limited in function. Signal changes induced by targeted MR CAs are generally small; and because protons are ubiquitous in all soft tissues of the body, there is substantial background signal that can render the changes in signal produced by the targeted probe undetectable. In addition, because many factors, both biological and equipment related, can result in changes in T_1 and T_2/T_{2*} relaxation, signal intensity changes in the final MR image can be difficult to interpret. A further complication can arise when a high concentration of IOs alter biological processes. Despite such challenges, great strides have been made over the last decade in the development of cancer-targeted MRI probes. This review will highlight the most significant of these and discuss their likely impact on the future of clinical cancer diagnosis.

Paramagnetic and Superparamagnetic MR Contrast Agents

All MR CAs, which differ greatly in size and structure (Fig. 1), provide information about organs, tissues, cells, and even extracellular and intracellular proteins and enzymes by causing signal intensity (brightness level) changes in MR images. Even without the use of CAs, MRI is a modality capable of producing many different patterns of contrast when imaging any given organ. Intrinsic contrast in the image depends on the concentration of protons in the tissue and their longitudinal (T1) and transverse (T2) relaxation times. MR scan parameters chosen during the exam, as well as the strength of the main magnetic field B_0, enhance or lessen the effect of these intrinsic variables to produce still greater variety in the signal intensities in the final image. Although somewhat daunting to beginning radiologists, it is precisely this capability that makes MRI such a powerful diagnostic tool since different diseases can be readily identified by their contrast characteristics across a panel of imaging sequences (T1 or T2-weighted, gradient echo (GE) and spin echo (SE), etc.) performed during the course of the exam. The addition of oral or injectable MR CAs merely builds on this level of analysis, offering yet one more way of generating selective contrast in the organ of interest. The paramagnetic metal Gd^{3+} carries seven unpaired electrons, which alter the local magnetic field experienced by surrounding protons and thereby speed their relaxation time (recovery of magnetization); this produces high (bright) signal in T1-weighted images. Chelation of Gd^{3+} by such molecules as diethylene triamine pentaacetic acid, (DTPA) renders the metal ion non-reactive with other biological tissue, thus minimizing metal induced toxicity in patients with normal renal function. The conjugation of Gd^{3+} chelates to proteins for the development of targeted MR CAs generally results in improving the metal's relaxivity, (i.e., the efficacy of contrast agent), by slowing

NIH-PA Author Manuscript

NIH-PA Author Manuscript

NIH-PA Author Manuscript

the tumbling rate of the paramagnetic complex [2]. Continued experimentation with newly developed targeted MR CAs will undoubtedly shed more light on the many ways in which the relaxivity of paramagnetic and superparamagnetic CA are altered through conjugation with proteins and by interactions with biomolecules *in vivo* [3].

Another class of MR CAs, superparamagnetic iron oxides (SPIO) are nanoparticles that consist of a core of ferric (Fe^{3+}) and ferrous (Fe^{2+}) iron in the form $Fe_2$3+OFe2+O that is surrounded by a layer of dextran or polysaccharide that keeps the iron particles from aggregating and improves their stability [4,5]. In the presence of an external magnetic field, the individual magnetic moments of IOs align producing a fluctuating magnetic field, which is large in comparison to that produced by gadolinium. SPIOs generally are used to generate contrast based on their ability to shorten T2 relaxation times (causing loss of signal on T2 or T2*-weighted MR images and hence 'negative contrast'), but they can also shorten T1 relaxation. Because SPIOs are more effective than Gd^{3+} in altering the relaxation of local protons, they can be used in lower concentrations and thus have an advantage over Gd^{3+}-based agents. They also have long blood retention times, are biodegradable, and have low toxicity profiles. Their properties can be adjusted by controlling the iron content of the core and the surface coatings (with the size of the iron core determining the magnetic properties of the agent, and the surface coatings determining the pharmacokinetics and excretion characteristics). Most importantly, SPIOs are ideally suited for attaching to carrier and targeting molecules, which gives them great utility for development as disease-targeted imaging probes (see [6,7]). A variety of approaches have been used to link cancer-targeting molecules to SPIOs (reviewed in [8]). SPIOs can be classified according to their size, with the larger agents having diameters of 20 to 3,500 nm (Ferumoxsil or AMI-121, Ferucarbotran, OMP), and ultrasmall SPIO (USPIO) agents having diameters of less than 50 nm (AMI-277, MION-47, Sinerem®, Combidex® (ferumoxtran-10), Clariscan™).

Perfusion-Based Tumor Detection

Although not a targeted imaging method per se, the use of Gd^{3+}-based CAs for detecting tumors warrants mentioning because of its historical importance in the development of MR CAs for oncologic imaging. The utility of using Gd^{3+}-based CAs for detecting tumors was recognized relatively early on [9] when it was realized that these agents could serve as perfusion tracers and thus could detect increased perfusion rates (and disruptions in the blood-brain-barrier) caused by neovascularization. Such changes often accompany tumor formation and the transition of cells into malignancy [10]. Once a tumor has grown larger than 2 – 3 mm, its need for nutrients exceeds that which can be provided by the existing vasculature. At this stage, tumor cells begin secreting a number of substances, including proteolytic enzymes and growth factors that act to modify the existing extracellular matrix and stimulate the growth of new vessels. Changes in perfusion resulting from the establishment of new vessels can be detected with the use of dynamic contrast-enhanced (DCE) MRI, a method in which a series of T1-weighted images are taken before, during, and after intravenous administration of a Gd^{3+}-based CA. During the 'wash-in' phase, the CA enters the highly vascularized tissue and the tissue appears as hyperintense, after which the agent leaves the tissue (wash-out phase) and the tissue returns to its original signal level. In some cases, the kinetics of the CA-induced signal change can be used to delineate benign from malignant tumors. DCE MRI (reviewed in [11] has been used successful for detecting tumors 1 – 2 mm and its use has contributed greatly to the acceptance of MRI as a standard diagnostic tool in oncology. In particular DCE has proven useful for detecting breast and prostate adenocarcinomas.

NIH-PA Author Manuscript

NIH-PA Author Manuscript

NIH-PA Author Manuscript

The Use of Non-Targeted MR CAs in Cancer Imaging

Whereas normal vessels restrict the passage of Gd^{3+} and IO-based CA, vessels in tumors are often more permeable and thus leak CA into the surrounding extravascular space, where it accumulates in the interstitial tissue compartment or is taken up by tumor cells (and other cells in the tumor microenvironment). The emergence of IO-based CAs for the detection of tumors began in the mid-1980's with the observation that tumors show up as hyperintense on T2-weighted images after systemic administration of IOs.[12,13,14] SPIOs are readily taken up by cells such as monocytes, macrophages, and oligodendroglial cells and enter into the cellular reticuloendothelial system (RES) of healthy liver, spleen and lymphatics, causing a loss in T2 signal in these tissues, while tumor cells that lack a functional RES fail to accumulate SPIOs and thus remain bright on T2-weighted images in relation to the surrounding normal tissue. The particles are stored in lysosomes (although some have been seen in cytoplasm and nucleus) until the carrier component (usually dextran) is excreted by the kidneys and the elemental iron enters the body's iron pool. In fact, the capacity of ferumoxytol. (Feraheme®, AMAG Pharmaceuticals, Lexington, MA) to treat iron deficiency is currently the only on-label use for this agent in the U.S. SPIOs have a long half-life in tumors (25–30 hours) due to the inefficient lymphatic drainage from these areas. SPIOs have been used to assess a variety of tumors in animals and humans (for reviews see [15,16]) and the development of these agents for more targeted imaging applications is underway as discussed below.

The utility of SPIOs and USPIOs for detection of metastatic disease was demonstrated in the early 1990s in animals,[17,18] and later in humans [19]. It is in this capacity that these agents have perhaps provided the greatest clinical value, as the determination of metastatic involvement of lymph nodes is key in cancer staging and therapeutic planning. SPIOs have been used to assess lymph node metastases in a large number of human cancer types with a great deal of success (reviewed in [20,21]), and guidelines for their use in this capacity have been established [22,23]. Although the use of SPIOs recently has been thwarted due to safety concerns, increases in the safety profile of new agents [24] should hasten the return of these agents to the clinic. Whereas IO-based agents delineate malignant nodes by their exclusion into these tissues, Gd^{3+}-based agents delineate nodal involvement by their sequestration into malignant nodes. Gd^{3+}-based agents, when carried through the systemic circulation, can permeate into thin-walled fenestrated lymphatic capillaries and subsequently be transported with lymphatic fluid to the lymph nodes. Because malignancy is often accompanied by insufficient lymphatic drainage, these agents accumulate in sentinel lymph nodes, causing the nodes to appear bright on T1-weighted images. Gd^{3+}-based CAs have been used with varying success over the last decade for detection of nodal metastasis [25]. Methods to enhance the MR detection of lymph nodes with Gd^{3+} have relied on the delivery of large payloads of Gd^{3+} chelates to the nodes via lipid carriers,[26] dendrimers, and micelles (e.g., perfluorocarbon-based paramagnetic micelles). [27]

The Use of Targeted MR CAs in Cancer Detection

Although perfusion-based MR methods such as DCE have proven effective in diagnosing tumors as small as 1–2 cm and conventional MR methods are still being improved for more accurate cancer detection and prognosis,[28,29] the sensitivity of these methods for detecting malignancy in its earliest stages, before gross anatomical changes have taken place, is lacking. In addition, conventional MRI methods frequently lack specificity for typing cancers for the purpose of differential diagnosis. Thus a concerted effort has been made to develop MR CAs that have the ability to detect even subtle changes in the intra and extracellular milieu during oncogenesis. The transformation of benign cells into malignancy is characterized by a concomitant array of biochemical changes in the microenvironment,

NIH-PA Author Manuscript

NIH-PA Author Manuscript

NIH-PA Author Manuscript

i.e., remodeling of the extracellular matrix, changes to the vascular endothelium, activation of inflammatory pathways and upregulation of cell surface proteins and enzymes involved in chemotaxis and adhesion. These changes provide ample potential targets for MR CA development.

Cells expressing a large number of binding sites accessible to targeting molecules can be potentially imaged using the systemic delivery of antibody- or non-antibody ligands either by injecting paramagnetic targeted agents directly into systemic circulation, or after pre-targeting the cancer-associated targeted sites with affinity molecules and injecting paramagnetic CA after the clearance of non-bound affinity molecules. In both cases, the imaging of cancer is improved by linking paramagnetic metals to large molecules, which have the inherent problem of nonspecific uptake and slow removal from circulation. Although the uptake by the cells of the reticuloendothelial system is a key characteristic in the utility of SPIOs as diagnostic agents, endocytosis/phagocytosis by professional phagocytes also removes nanoparticles from the circulation, thus preventing them from reaching specific cellular targets. Fortunately, the level of SPIO opsonization in blood, and thus the macrophage uptake and blood half-life of these agents, can in most cases be altered by changing the coating layer of the nanoparticles. It has been reported that low hydrophobicity of the surface and/or negative surface charge can hinder rapid phagocytosis and clearance from the circulation after intravenous injections.

The greatest limiting factor in the development of cell or receptor-targeted MR CAs is sensitivity. Even in the case of receptors, which are greatly overexpressed in cancerous cells, the ability to link sufficient quantities of CA to the target to produce a detectable contrast change in the MR image is limited. Early attempts to detect Gd^{3+} chelates linked to monoclonal antibodies (mAb) targeted against cell surface receptors were unsuccessful due to the limited number of Gd^{3+} ions per antibody [30,31,32]. It is estimated that local concentrations of Gd^{3+} must be in the range of 10 to 500 uM to produce detectable contrast enhancements [33,6], which translates into a substantial number (greater than 10) of Gd^{3+} ions per mAb even if the antigen (i.e., a cell surface receptor) is highly expressed in the tissue.

In some cases, the problem of sensitivity can be addressed by designing CAs that are taken up via passive or receptor-mediated transport into the cells of interest, thus providing an avenue for accumulation of the probe. Continued development of carrier molecules for paramagnetic agents such as micelles, liposomes, micro-emulsions, apoferritin, and lipoproteins further increase the potential for MRI of cancer targets that exist in low concentration in tumors and pre-malignant cells.

Another approach that has been used to deliver higher concentrations of Gd^{3+}-chelates to tumors is the use of dendrimers. Dendrimers are synthetic molecules that consist of a core surrounded by concentric shells (termed generations) made up of covalently linked branched chemical moieties. Moieties in the outer shell can serve as attachment points for functional groups, substrates, or CAs. In most cases, the linking of chelated Gd^{3+} to dendrimeric carriers increases relaxivity of the metal, resulting in greater signal enhancement in the MR image (reviewed in [34]). Aptamers (DNA or RNA oligonucleotides) also have been used as cancer targeting agents for conjugation to IOs and are well suited for this purpose due to their low molecular weights, lack of immunogenicity, and availability. Hwang do et al.[35] developed a multimodality imaging probe (for concurrent fluorescence, radionuclide and MRI) based on a cobalt-ferrite nanoparticle bound to the cancer-specific aptamer, AS1411. Twenty-four hours after intravenous administration to nude mice bearing C6 tumors, T2-weighted MR images could be clearly visualized as black spots, whereas no change in signal was seen for control injected animals.

NIH-PA Author Manuscript

NIH-PA Author Manuscript

NIH-PA Author Manuscript

Although Gd-linked dendrimers or IO nanoparticles can localize greater amounts of CA to a tissue, alternative strategies have been sought to increase the target to background/contrast ratio produced by these agents. 'Activatable', or 'amplifiable' (MRamp) agents rely on the activity of endogenous or exogenous enzymes or other biomolecules to chemically modify the CA after it has bound its target, thereby causing the CAs to be retained in the tissue of interest (i.e., a tumor).

Our laboratory has demonstrated a method whereby a low molecular weight MRamp agent, di- 5-hydroxytryptamide of DTPA(Gd) (5-HT) is caused to oligomerize and accumulate at the site of xenografted A431 tumors (human squamous cell carcinoma) after the 5HT substrate is oxidized by exogenous horseradish peroxidase (HRP). [36,37] HRP (and the catalyst glucose oxidase) is selectively brought to the site of the tumor by linking it to the tumor-specific monoclonal antibody (anti-L6 mAb) that binds the Lewis Y antigen overexpressed in many carcinomas (Fig. 2). Using this technique, we observed a stronger regional enhancement of tumors over a longer time span (a 160% increase at approx. at 55 min post contrast) in experimental animals than in control ones. In this case, the relaxivity changes were due to the activation of bis-5HT- DTPAGd by peroxidases and accumulation at the site of antibody binding as a result of oligomerization and binding to tyrosine-containing proteins. Enzymatic MR CA signal amplification has shown great promise for detecting malignancies in animal models of cancer, especially in instances where only a small number of malignant cells are present, or when the cancer-specific target (such as a receptor) exists at a low concentration.

A different approach that has been used to amplify the signal generated by extremely low concentration molecular targets is paramagnetic chemical exchange saturation technique (PARACEST) [38]. In this technique, protons in direct contact with the target CA molecule are saturated (made 'MR silent') by a selective radiofrequency pulse. The ensuing transient loss of signal is then transferred to nearby protons because of inhomogeneities created in the surrounding environment.

Targeting Neovascularization

Because pathological angiogenesis is a critical event in the initiation and maintenance of tumor growth, biomolecules involved in neovascularization are considered to be ideal targets for tumor detection strategies. The role of endothelial $\alpha_5\beta_3$ integrin in aberrant vessel growth has been firmly established and its concentration has been shown to correlate with tumor grade grade [39]. Integrin $\alpha_5\beta_3$ binds to the peptide sequence arginine-glycine-aspartic acid (RGD), and disruption of integrin-mediated signaling inhibits angiogenesis [40] and slows tumor growth progression. In an early study, Sipkins et al [41] reported the use of polymerized paramagnetic liposomes for delivery of gadolinium to endothelial $\alpha_v\beta_3$ expression in a rabbit model of squamous cell carcinoma. Avidin conjugated liposomes were localized to $\alpha_v\beta_3$ via linking to biotinylated anti $\alpha_v\beta_3$ monoclonal antibodies, allowing for MR contrast enhancement of tumors and visualization of hot spots of tumor angiogenesis. A similar approach in which Gd-chelates were contained in perfluocarbon nanoparticles linked to $\alpha_5\beta_3$ antibodies was used to image neovascularization in rabbit cornea [42]. In this study, a 25% increase in signal intensity was seen after CA administration. Most recently, the technique has been used with ^{99m}Tc-labeled nanoparticles carrying Gd-chelates for multimodality (SPECT-CT and MR) molecular imaging and 3D neovascular mapping [43]. In a slightly different approach, Ke et al. [44] used Gd-DO3A conjugated to Cyclic Arg-Gly-Asp-D-Phe-Lys to target $\alpha_v\beta_3$ integrin in nude mice implanted with DU145 xenografts to model human prostate cancer. In this study, decreases in T1 relaxation (and subsequent T1-mapping) were used to delineate tumor margins.

NIH-PA Author Manuscript

NIH-PA Author Manuscript

NIH-PA Author Manuscript

IO-based MR probes have also been targeted to $\alpha_5\beta_3$ integrin. In 2007, Zhang et al. [45] conjugated USPIOs with Arg-Gly-Asp (RGD) peptides, which are known to bind to $\alpha_5\beta_3$ integrin receptors, and tested the ability of this agent to distinguish between high and low expressing $\alpha_5\beta_3$ integrin tumors in nude mice. Not only did the increase in T2 relaxation correlate with the amount of $\alpha_5\beta_3$ integrin expression (higher expressing tumors showed greater shortening of T2 relaxation times), but the agent produced a visually distinguishable contrast pattern in the two tumor types with the high $\alpha_5\beta_3$ integrin expressing tumors showing irregular signal intensity decreases and the lower $\alpha_5\beta_3$ integrin expressing tumors showing a more homogenous decrease in signal. Lee et al. [46] developed a bifunctional $\alpha_5\beta_3$ integrin target MRI/PET probe by using polyaspartic acid (PASP)-coated IO (PASP-IO) nanoparticles, which were also labeled with ^{64}Cu. The probe was useful for detecting decreased signal intensity in T2-weighted images of mice bearing U87MG tumors, and was also accumulated in the RES of the liver and spleen. An $\alpha_5\beta_3$ integrin targeted dual MR and near-infrared fluorescent (NIRF) probes have also been developed and tested in vivo in a subcutaneous U87MG glioblastoma model [47].

Another molecule that is highly expressed during injury and neovascularization is E-selectin, an adhesion molecule bound to endothelium that serves in recruiting and anchoring leukocytes to the endothelial wall, where they subsequently enter the tissue interstitium to initiate an immune response. We first developed and demonstrated an MR nanoprobe that consisted of covalent conjugates of cross-linked iron oxide nanoparticles (CLIO) and high-affinity (*K*d app= 8.5 nM) anti-human E-selectin (CD62E) F(ab')$_2$ fragments [48]. When incubated in the presence of IL-1β (which induces E-selectin expression in endothelial cells) *in vitro*, the probe showed selective binding to human endothelial umbilical vein cells (HUVEC) and engineered human blood vessels *in vivo* and produced a significant specific T2-weighted signal in implants seeded with human endothelial cells [49].

Reynolds et al.[50] conjugated anti-murine E-selectin F(ab')$_2$ monoclonal antibody fragment to USPIOs that could then be detected on T2-weighted MR images in areas of localized inflammation in mice. In a slightly different approach, Boutry and colleagues targeted USPIOs to sites of inflammation and E-selectin expression by conjugating the USPIOs to a synthetic analog of sialyl Lewis(x) [sLe(x)], a natural ligand of E-selectin [51]. Although use of E-selectin targeted molecules for the direct *in vivo* MRI of tumors has not been reported, this application is undoubtedly underway.

Targeting the Extracellular Matrix

Matrix metalloproteinases (MMPs) have been extensively investigated in animal models of cancer as candidates for "smart" enzyme-sensitive MRI probes since MMPs degrade extracellular matrix in lieu of tissue remodeling, which occurs in both normal and pathological conditions.[52] In order to generate specific MR contrast in areas of MMP-7 activity, Lepage et al. conjugated MMP substrates to Gd-DOTA that had been modified by linking to a solubility enhancing moiety. Upon binding of the substrate to MMP-7, the hydrophilic portion of the CA was cleaved, thereby producing an insoluble Gd-DOTA molecule that was then trapped (and thus accumulated) in the tissue at sites of high MMP-7 activity [53]. MMP-2 and MMP-9 have also been targeted for molecular MRI applications. Dendrimers carrying up to 30 Gd-DOTA moieties, and coated with activatable *Antennapedia* homeobox protein cell penetrating peptides (CPPs) were made activatable by linking CCPs to an inhibitory domain consisting of negatively charged amino acid residues. Cleavage of the linker between the polycationic and polyanionic domains, in this case by MMP-2 and MMP-9, released the CPP portion and allowed the Gd^{3+} linked dendrimer to be taken up into tumors in rats [54]. Once activated, the Gd-labeled nanoparticles deposited high levels (30 – 50 μM) of Gd in tumor parenchyma, with even higher amounts deposited in

NIH-PA Author Manuscript

NIH-PA Author Manuscript

NIH-PA Author Manuscript

regions of infiltrative tumor, resulting in detectable T1 contrast lasting several days after injection.

The extracellular matrix molecules fibrin and fibronectin, associated with intermediary and high tumor malignancy, have also been targeted for molecular MR CA development. Gd-DTPA directly conjugated to CLT1 [55], results in a peptide sequence that binds with high affinity to fibrin-fibronectin complexes in tumor stroma, or to lysine dendrimers [56]. This MR sensitive peptide sequence was shown to significantly increase contrast in female athymic mice bearing MDA-MB-231 human breast carcinoma xenografts or mice bearing HT-29 human colon carcinoma xenografts for up to 1 h post injection, whereas nontargeted Gd-DTPA was cleared rapidly and showed only non-specific, transient enhancement.

Targeting Cell Death

Cell death (apoptosis) is a consequence of tumorigenesis, and can serve as an indicator of malignant progression. Producing apoptosis in tumors is also a goal of radiation and cytotoxic chemotherapies, and thus molecular MR probes that recognize apoptosis can serve to define tumors and to assess the efficacy of treatment regimens. Several molecular biomarkers of apoptotic cells have been investigated as candidates for MR probe development. Both annexin V and the C2 domain of synaptotagmin I bind phosphatidylserine residues in the plasma membranes of apoptotic cells, and have been linked to IOs or Gd^{3+}-chelates [57,58] to detect response to chemotherapeutic drugs[59], and for *in vivo* detection of apoptosis induced by chemotherapeutic drugs (e.g. camptothecin or etopoposide) [60]. van Tilborg and colleagues [61] have tested *in vitro* annexin A5-conjugated lipid carrier agents (pegylated micelles/liposomes) as delivery systems for IOs and Gd chelates to apoptotic cells. More recently, gadolinium p-aminobenzyl-diethylenetriaminepentaacetic acid-poly(glutamic acid) (L-PG-DTPA-Gd and D-PG-DTPA-Gd), was shown to accumulate in human Colo-205 xenograft and syngeneic murine OCA-1 ovarian tumors, following the initiation of necrosis by poly(L-glutamic acid)-paclitaxel conjugate (PG-TXL). Although the initial enhancement of tumor after injection of L-PG-DTPA-Gd and D-PG-DTPA-Gd was low compared to that produced by low molecular weight contrast agents, the enhancement was long-lasting, allowing necrotic tissue to be clearly distinguished from surrounding tissue. The localization of L-PG-DTPA-Gd suggests that the accumulation in necrotic tissue was mediated via phagocytic uptake into macrophages.

Targeting Cell Surface Receptors

Liver Cancer

One of the first reported uses of targeted IO CAs in an animal model of cancer described the MR differentiation of malignant and normal cells of the liver by imaging arabinogalactan (AG)-linked USPIOs in mice [62, 63]. AG is a galactose-terminated glycoprotein that recognizes asialoglycoprotein (ASG) receptors on hepatocytes. Intravenous administration of AG-USPIO caused shorter T2 relaxation times in normal liver as compared to malignant hepatocellular carcinoma cells, which are poor phagocytes, lack functional ASG receptors, and failed to take up AG-USPIO. This resulted in “bright” T2-weighted images of carcinomas on the background of dark normal liver tissue. In a more recent study, hepatic tumors in rats were detected by mesenchymal-epithelial transition factor (c-MET) conjugated IOs [64]. Activation of c-MET has been implicated in the formation of several cancers, including hepatocellular carcinomas. The probe could detect overexpression of c-MET in neoplastic nodules and tumors within the livers of CDAA-treated rats, as determined by a decrease in MRI signal intensity and a decrease in regional T2 values.

NIH-PA Author Manuscript

NIH-PA Author Manuscript

NIH-PA Author Manuscript

Pancreatic Cancer

In an early attempt to image pancreatic tumors, Reimer et al. [65] reported targeting monocrystalline iron oxide (MION) to rat pancreas by linking cholecystokinin (CCK), a peptide hormone that binds to a G-protein coupled receptor expressed in high numbers on pancreatic acinar cells, to USPIO. The binding of the CCK-MION was shown to be both specific and saturable. Shen et al.[66], imaged pancreatic tumors by targeting secretin receptors on normal pancreatic acinar cells. In this study the secretin receptors were first tagged with biotin, and were then recognized by strepavidin-MION conjugates. More recently, Yang et al. reported the development of an IO-based MR probe for the detection of pancreatic cancer [67]. In this study nanoparticles (either IO or quantum dots) were conjugated to a single-chain anti-EGFR antibody (ScFvEGFR), which allowed internalization of the probe in EGFR-expressing pancreatic cancer cells after administration in nude mice. An almost five-fold reduction in the MR signal was seen in tumors after the injection of ScFvEGFR-IOs but not in the case of non-targeted nanoparticles. A reverse “negative” targeting strategy was used in Montel et al.[68] for MR imaging of an animal model of pancreatic ductal adenocarcinoma (PDAC). Most of the ligands previously used for molecular probe development (somatostatin, secretin, bombesin, CCK, VIP) are unsuitable for imaging pancreatic tumors because normal pancreas expresses these molecules. The authors made use of the fact that bombesin (BN) receptors are expressed in sufficient quantities on normal pancreatic acinar cells but are lacking in pancreatic cancer [69]. In addition, BN receptors internalize ligands, suggesting that BN targeted nanoparticles might be selectively taken up in normal pancreas. A BN peptide-nanoparticle conjugate, BN-CLIO(Cy5.5), was found to accumulate in normal mouse pancreas in receptor-dependent fashion and to decrease T2 relaxation times, resulting in a darkening of normal pancreas on T2-weighted MR images. In comparison, tumors induced from a pancreatic tumor cell line, MIA-PaCa2, became readily visible with well-defined borders.

Prostate Cancer

Internalization and accumulation of Gd^{3+} in prostate cancer cells has been accomplished by linking Gd-DOTA to an antisense oligonucleotide sequence and a transmembrane carrier peptide [70]. The carrier peptide is included for delivering CA into the cell cytoplasm and the antisense oligonucleotide supposedly targets the CA to the nucleus to the site of c-myc mRNA, which is overexpressed in prostate cancer cells.

Ovarian Cancer

In a series of studies by Wiener and colleagues, Gd-DTPA covalently linked to four generation polyamidoamine (PAMAM) dendrimers were targeted to ovarian adenocarcinoma by conjugation to folate. Folate is essential for DNA synthesis in rapidly dividing cells and folate receptor alpha is overexpressed in many adenocarcinomas. Following *in vivo* administration in nude mice bearing ovarian tumor xenographs, accumulation of the CA at the tumor site resulted in a 33% contrast enhancement which was not obtained post administration of a non-specific agent, or in folate-receptor negative tumors. Contrast enhancement could be blocked by administration of free folic acid, suggesting that the enhancement was dependent on accumulation of the CA via folate-receptor mediated binding [71].

Breast Cancer

One of the earliest attempts to develop an MR CA for selective imaging of breast cancer used USPIOs covalently linked to transferring [72]. The transferrin receptor (TfR) is overexpressed in many types of cancer [73,74], and is particularly attractive for targeted MR probe development due to its capability to enter and accumulate in cells. Transferrin linked

NIH-PA Author Manuscript

NIH-PA Author Manuscript

NIH-PA Author Manuscript

USPIOs were able to generate tumor specific MR contrast (40% reduction in signal on T2-weighted images) in a rat model of breast cancer. In a different approach, the high affinity binding of avidin to biotin was used for targeting MR detectable probes to the HER-2/neu receptor [75]. A member of the epidermal growth factor (EGF) family of Erb transmembrane tyrosine kinase receptors, it has been shown to be upregulated in breast cancer [76]. Tumors pre-labeled using an injection of biotinylated anti- HER-2/neu antibody, were easily detected in T1-weighted images in an *in vivo* model of breast cancer after systemic administration of avidin labeled an GdDTPA–avidin conjugate 12 h later [75].

Huh et al. [77] synthesized iron oxide nanocrystals, made them water soluble by attachment to 2,3-dimercaptosuccinic acid (DMSA), and then conjugated them to Herceptin antibody. An animal model of breast cancer was devised by implantation of human NIH3T6.7 cell lines overexpressing HER2/*neu* into mice hind leg. Color mapping of T2 and T2*-weighted MR images taken at 9T from mice implanted with, showed an immediate (within 5 minutes) increase of tissue relaxation rates at the border of the tumor followed by a more gradual increase encompassing 2/3 of the tumor by 12 h post injection. In 2007, the same group developed magnetism-engineered iron oxide (MEIO) nanoparticles, which were uniform in size, showed single crystallinity, and had a very pronounced supermagnetism.[78] These agents demonstrated enhanced MRI sensitivity when conjugated with Herceptin antibodies and used to detect cancer in mice. Their results indicated that MnMEIO-herceptin conjugates enabled the detection of tumors as small as ~ 50 mg. Conjugation of Herceptin to SPIOs at a concentration of 20 μmol/kg has also been demonstrated to have utility in detection of breast tumor allografts *in vivo*, and has shown MR enhancement that increases proportionally with the level of HER2/neu expression in tumors [79].

Another molecule that has been tested for cancer-targeted MR imaging *in vivo* is luteinizing hormone releasing hormone (LHRH) [80]. Iron oxide nanoparticles that were conjugated to LHRH and luteinizing hormone/chorionic gonadotropin (LH/CG) showed high affinity binding to human breast cancer cells *in vitro* but were poorly taken up by macrophages. *In vivo* LHRH-IO specifically accumulated in the cytosolic compartment of xenografted human breast cancer cells. Iron oxides were also found in lung metastatic lesions. Another successful method of imaging mammary tumors in animals was reported by Yang et. al. [81], who used a recombinant peptide containing the amino-terminal fragment (ATF) of urokinase type plasminogen activator (uPA) conjugated to magnetic ironoxide nanoparticles. uPA is an attractive candidate for imaging probe development because it is a predictor of tumor aggressiveness, metastasis, and poor prognosis in breast cancer patients. In this study, ATF-IO nanoparticles were shown to bind to and be internalized by uPA receptor expressing tumor cells, after systemic delivery of ATF-IO into mice bearing subcutaneous and intraperitoneal mammary tumors. This selective uptake was followed by a three-fold signal decrease in T2-weighted images in various areas of the tumor mass – an effect that was absent in the case control non-targeted iron oxide particles. Signal decreases were also seen in tumor metastases in these animals. Other molecules associated with breast cancer have also been targeted for MR probe development. Somatostatin receptors (SSTRs) are also highly expressed on breast cancer cells and have been targeted using Octreotide-conjugated USPIOs [82]. After targeted USPIO were injected in mice xenografted with breast adenocarcinoma, tumor signal intensity gradually decreased with the corresponding T2 value decrease by 24.5% of the initial T2, while T2 values in control tissue declined to 22%.

CNS Tumors

Veisheh et al. [83] overcame the problem of limited transport of IOs across the tumor-compromised blood brain barrier (BBB) by coating IO nanoparticles with a polyethylene glycol (PEG) grafted chitosan copolymer. The CA was then conjugated to cholorotoxin, a peptide that binds to matrix metalloproteinase 2 (MMP-2) isoforms selectively expressed in

NIH-PA Author Manuscript

NIH-PA Author Manuscript

NIH-PA Author Manuscript

gliomas. Two days after injection of the probe (NPCP-CTX) into mice bearing cerebellar tumors, relaxivity ($1/T_2$) measurements showed that tumors exhibited a much higher R_2 value of 472.3 $s^{-1}mmol/L^{-1}$ whereas non-conjugated IO exhibited values of 243.3 $s^{-1}mmol/L^{-1}$. No such R_2 changes were found in normal brain tissues of tumor-bearing or control animals, and unmodified IOs did not produce R_2 changes in tumors. In addition, histological analysis determined that passage of the nanoprobe had not compromised the integrity of the BBB, suggesting that this probe may be an ideal candidate for further testing in humans.

We have used MRamp technique to detect the overexpression of epidermal growth factor (EGF) receptor in a mouse model of neuroglioma [84,85] and human squamous carcinoma [86]. Overexpression of EGFR is implicated in the development of aggressive gliomas. In addition to the MRamp agent producing a strong signal enhancement at the tumor site, it changed the kinetics of elimination of the CA and also a differential pattern of enhancement in the tumor (Fig. 3). When imaged after substrate alone, the temporal dynamics of MR signal elimination from the tumor showed that almost no MRI contrast remained after 24h. Alternatively, when imaged after the preinjection with EGFR-targeted antibody conjugates, the temporal dynamics of T1-signal enhancement and contrast agent retention in the tumor margin (Fig. 3) was significantly increased at 2.5 hours and at later time points (up to 24 h) after the injection. Immunohistochemical corroboration revealed that the spatial distribution of EGFR overexpression closely resembled the pattern of T1-signal enhancement in the tumors. EGFR-positive tumor margin was positive for markers of angiogenesis and glucose oxidase (the evidence of conjugate delivery), whereas no enhancement of the tumor margin was observed in control tumors, which do not overexpress EGFR [87].

Other Targeting Molecules

Iron oxides have also been chemically modified to target a number of other cancer specific molecules in animal models including MUC-1. Underglycosylated mucin-1 antigen (uMUC-1) is overexpressed in over 50% of all human cancers, and its expression remains up-regulated throughout the course of malignancy and metastatic progression. [88] Moore et al. linked EPPT1, a synthetic peptide derived from a monoclonal antibody (ASM2) raised against human epithelial cancer cells[89], to the aminated crosslinked dextrans of iron oxide (CLIO) nanoparticles. Cy5.5 was also linked to the same particles for dual MR and NIRF detection of uMUC-1 positive tumors in mice. Twenty four hours after injection of the CLIO-EPPT probe (10 mg Fe/kg), T2-weighted MR images revealed no significant changes in signal intensity in μMUC-1-negative tumors, while a significant signal reduction (up to 53%) was observed in animals bearing uMUC-1-positive tumors (Fig. 4). The uMUC-1-positive tumors could also be detected by NIRF. In a more recent study, the same group [90] showed the utility of this approach in the MR evaluation of tumor volume reduction after doxorubicin treatment in mice bearing orthotopic human breast carcinomas. Folate receptors have also been used for molecular MR imaging of *in vivo* animal models of cancer. In one of the first of such reports, Choi et al.[91] showed an average intensity decrease of 38% produced by folate targeted IO particles. The mechanism of action was believed to be endocytosis mediated internalization of nanoparticles into tumor cells.

Future Directions

Recent advances in chemistry and nanotechnology prove promising for the continued development of highly sensitive molecular MR probes for early detection of cancer and other diseases. Wide scale molecular screening approaches have the potential to identify a number of novel targeting ligands that would be candidates for MR probe development [92]. In addition, improved methods for increasing imaging sensitivity and specificity should render existing probes more applicable to detecting even lower concentration of targets *in*

NIH-PA Author Manuscript

NIH-PA Author Manuscript

NIH-PA Author Manuscript

vivo. Novel synthetic CAs with enhanced magnetic properties are essential for increasing the sensitivity of imaging. Lee et al. [93,94] have developed FeCo-graphitic carbon shell nanocrystals that allow microvessels as small 100 μm to be imaged at 1.5T. Another direction is the development of multimodality imaging probes as well as agents that act as simultaneous detectors and therapeutic/drug delivery agents for cancers.[95,96,97] Finally, the combined use of multiple MR contrast generating techniques should also enable the MR detection of multiple molecular targets simultaneously, allowing even greater diagnostic capabilities in oncology.

References

1. J M New cancer cases will grow 30% by 2020. Economist Intelligence Unit; 2009. Available from www.eiu.com
2. Caravan P. Protein-targeted gadolinium-based magnetic resonance imaging (MRI) contrast agents: design and mechanism of action. Acc Chem Res. 2009; 42:851–62. [PubMed: 19222207]
3. Hanaoka K, Lubag AJ, Castillo-Muzquiz A, Kodadek T, Sherry AD. The detection limit of a Gd3+-based T1 agent is substantially reduced when targeted to a protein microdomain. Magn Reson Imaging. 2008; 26:608–17. [PubMed: 18234462]
4. Koenig SH, Baglin CM, Brown RD 3r. Magnetic field dependence of solvent proton relaxation in aqueous solutions of Fe^{3+} complexes. Magn Reson Med. 1985; 2:283–8. [PubMed: 3938511]
5. Renshaw PF, Owen CS, McLaughlin AC, Frey TG, Leigh JS Jr. Ferromagnetic contrast agents: a new approach. Magn Reson Med. 1986; 3:217–25. [PubMed: 3713487]
6. Geraldes CF, Laurent S. Classification and basic properties of contrast agents for magnetic resonance imaging. Contrast Media Mol Imaging. 2009; 4:1–23. [PubMed: 19156706]
7. Lin MM, Kim HH, Kim H, Dobson J, Kim do K. Surface activation and targeting strategies of superparamagnetic iron oxide nanoparticles in cancer-oriented diagnosis and therapy. Nanomedicine (Lond). 2010; 5:109–33. [PubMed: 20025469]
8. Elias DR, Thorek DL, Chen AK, Czupryna J, Tsourkas A. In vivo imaging of cancer biomarkers using activatable molecular probes. Cancer Biomark. 2008; 4:287–305. [PubMed: 19126958]
9. Wesbey GE, Engelstad BL, Brasch RC. Paramagnetic pharmaceuticals for magnetic resonance imaging. Physiol Chem Phys Med NMR. 1984; 16:145–55. [PubMed: 6095341]
10. Jensen HM, Chen I, DeVault MR, Lewis AE. Angiogenesis induced by “normal” human breast tissue: a probable marker for precancer. Science. 1982; 218:293–5. [PubMed: 6181563]
11. Pathak AP. Magnetic resonance susceptibility based perfusion imaging of tumors using iron oxide nanoparticles. Wiley Interdiscip Rev Nanomed Nanobiotechnol. 2009; 1:84–97. [PubMed: 20049781]
12. Saini S, Stark DD, Hahn PF, Wittenberg J, Brady TJ, Ferrucci JT Jr. Ferrite particles: a superparamagnetic MR contrast agent for the reticuloendothelial system. Radiology. 1987; 162:211–6. [PubMed: 3786765]
13. Saini S, Stark DD, Hahn PF, Bousquet JC, Introcasso J, Wittenberg J, et al. Ferrite particles: a superparamagnetic MR contrast agent for enhanced detection of liver carcinoma. Radiology. 1987; 162:217–22. [PubMed: 3786766]
14. Weissleder R, Hahn PF, Stark DD, Elizondo G, Saini S, Todd LE, et al. Superparamagnetic iron oxide: enhanced detection of focal splenic tumors with MR imaging. Radiology. 1988; 169:399–403. [PubMed: 3174987]
15. Peng XH, Qian X, Mao H, Wang AY, Chen ZG, Nie S, et al. Targeted magnetic iron oxide nanoparticles for tumor imaging and therapy. Int J Nanomedicine. 2008; 3:311–21. [PubMed: 18990940]
16. Islam T, Harisinghani MG. Overview of nanoparticle use in cancer imaging. Cancer Biomark. 2009; 5:61–7. [PubMed: 19414922]
17. Weissleder R, Elizondo G, Josephson L, Compton CC, Fretz CJ, Stark DD, et al. Experimental lymph node metastases: enhanced detection with MR lymphography. Radiology. 1989; 171:835–9. [PubMed: 2717761]

NIH-PA Author Manuscript

NIH-PA Author Manuscript

NIH-PA Author Manuscript

18. Weissleder R, Elizondo G, Wittenberg J, Lee AS, Josephson L, Brady TJ. Ultrasmall superparamagnetic iron oxide: an intravenous contrast agent for assessing lymph nodes with MR imaging. Radiology. 1990; 175:494–8. [PubMed: 2326475]
19. Anzai Y, Blackwell KE, Hirschowitz SL, Rogers JW, Sato Y, Yuh WT, et al. Initial clinical experience with dextran-coated superparamagnetic iron oxide for detection of lymph node metastases in patients with head and neck cancer. Radiology. 1994; 192:709–15. [PubMed: 7520182]
20. Klerkx WM, Bax L, Veldhuis WB, Heintz AP, Mali WP, Peeters PH, et al. Detection of lymph node metastases by gadolinium-enhanced magnetic resonance imaging: systematic review and meta-analysis. J Natl Cancer Inst. 2010; 102:244–53. [PubMed: 20124189]
21. Will O, Purkayastha S, Chan C, Athanasiou T, Darzi AW, Gedroyc W, et al. Diagnostic precision of nanoparticle-enhanced MRI for lymph-node metastases: a meta-analysis. Lancet Oncol. 2006; 7:52–60. [PubMed: 16389184]
22. Saksena MA, Saokar A, Harisinghani MG. Lymphotropic nanoparticle enhanced MR imaging (LNMRI) technique for lymph node imaging. Eur J Radiol. 2006; 58:367–74. [PubMed: 16472955]
23. Lahaye MJ, Engelen SM, Kessels AG, de Bruine AP, von Meyenfeldt MF, van Engelshoven JM, et al. USPIO-enhanced MR imaging for nodal staging in patients with primary rectal cancer: predictive criteria. Radiology. 2008; 246:804–11. [PubMed: 18195379]
24. Bernd H, De Kerviler E, Gaillard S, Bonnemain B. Safety and tolerability of ultrasmall superparamagnetic iron oxide contrast agent: comprehensive analysis of a clinical development program. Invest Radiol. 2009; 44:336–42. [PubMed: 19661843]
25. Misselwitz B. MR contrast agents in lymph node imaging. Eur J Radiol. 2006; 58:375–82. [PubMed: 16464554]
26. Moghimi SM, Bonnemain B. Subcutaneous and intravenous delivery of diagnostic agents to the lymphatic system: applications in lymphoscintigraphy and indirect lymphography. Adv Drug Deliv Rev. 1999; 37:295–312. [PubMed: 10837741]
27. Choi SH, Han MH, Moon WK, Son KR, Won JK, Kim JH, et al. Cervical lymph node metastases: MR imaging of gadofluorine M and monocrystalline iron oxide nanoparticle-47 in a rabbit model of head and neck cancer. Radiology. 2006; 241:753–62. [PubMed: 17032913]
28. Galban CJ, Chenevert TL, Meyer CR, Tsien C, Lawrence TS, Hamstra DA, et al. The parametric response map is an imaging biomarker for early cancer treatment outcome. Nat Med. 2009; 15:572–6. [PubMed: 19377487]
29. Zong Y, Wang X, Jeong EK, Parker DL, Lu ZR. Structural effect on degradability and in vivo contrast enhancement of polydisulfide Gd(III) complexes as biodegradable macromolecular MRI contrast agents. Magn Reson Imaging. 2009; 27:503–11. [PubMed: 18814987]
30. Unger EC, Totty WG, Neufeld DM, Otsuka FL, Murphy WA, Welch MS, et al. Magnetic resonance imaging using gadolinium labeled monoclonal antibody. Invest Radiol. 1985; 20:693–700. [PubMed: 4066240]
31. Matsumura A, Shibata Y, Nakagawa K, Nose T. MRI contrast enhancement by Gd-DTPA-monoclonal antibody in 9L glioma rats. Acta Neurochir Suppl (Wien). 1994; 60:356–8. [PubMed: 7976589]
32. Shahbazi-Gahrouei D, Williams M, Rizvi S, Allen BJ. In vivo studies of Gd-DTPA-monoclonal antibody and gd-porphyrins: potential magnetic resonance imaging contrast agents for melanoma. J Magn Reson Imaging. 2001; 14:169–74. [PubMed: 11477676]
33. Pathak AP, Gimi B, Glunde K, Ackerstaff E, Artemov D, Bhujwalla ZM. Molecular and functional imaging of cancer: advances in MRI and MRS. Methods Enzymol. 2004; 386:3–60. [PubMed: 15120245]
34. Longmire M, Choyke PL, Kobayashi H. Dendrimer-based contrast agents for molecular imaging. Curr Top Med Chem. 2008; 8:1180–6. [PubMed: 18855704]
35. Hwang do W, Ko HY, Lee JH, Kang H, Ryu SH, Song IC, et al. A nucleolin-targeted multimodal nanoparticle imaging probe for tracking cancer cells using an aptamer. J Nucl Med. 2010; 51:98–105. [PubMed: 20008986]

NIH-PA Author Manuscript

NIH-PA Author Manuscript

NIH-PA Author Manuscript

36. Bogdanov A Jr, Matuszewski L, Bremer C, Petrovsky A, Weissleder R. Oligomerization of paramagnetic substrates result in signal amplification and can be used for MR imaging of molecular targets. Mol Imaging. 2002; 1:16–23. [PubMed: 12920857]
37. Bogdanov, A.; Kang, HW.; Bennett, DG.; Querol, Sans M.; Yudina, A.; Verel, I., et al. Tumor-targeted enzyme mediated MR signal amplification using paramagnetic substrates [abstract]. Proc. Intl Soc Magn Reson Med (Meeting Abstracts); 2006. p. 685
38. Zhang S, Merritt M, Woessner DE, Lenkinski RE, Sherry AD. PARACEST agents: modulating MRI contrast via water proton exchange. Acc Chem Res. 2003; 36:783–90. [PubMed: 14567712]
39. Ruoslahti E. Specialization of tumour vasculature. Nat Rev Cancer. 2002; 2:83–90. [PubMed: 12635171]
40. Cai W, Chen X. Anti-angiogenic cancer therapy based on integrin alphavbeta3 antagonism. Anticancer Agents Med Chem. 2006; 6:407–28. [PubMed: 17017851]
41. Sipkins DA, Cheresh DA, Kazemi MR, Nevin LM, Bednarski MD, Li KC. Detection of tumor angiogenesis in vivo by alphaVbeta3-targeted magnetic resonance imaging. Nat Med. 1998; 4:623–6. [PubMed: 9585240]
42. Anderson SA, Rader RK, Westlin WF, Null C, Jackson D, Lanza GM, et al. Magnetic resonance contrast enhancement of neovasculature with alpha(v)beta(3)-targeted nanoparticles. Magn Reson Med. 2000; 44:433–9. [PubMed: 10975896]
43. Lijowski M, Caruthers S, Hu G, Zhang H, Scott MJ, Williams T, et al. High sensitivity: high-resolution SPECT-CT/MR molecular imaging of angiogenesis in the Vx2 model. Invest Radiol. 2009; 44:15–22. [PubMed: 18836386]
44. Ke T, Jeong EK, Wang X, Feng Y, Parker DL, Lu ZR. RGD targeted poly(L-glutamic acid)-cystamine-(Gd-DO3A) conjugate for detecting angiogenesis biomarker alpha(v) beta3 integrin with MRT, mapping. Int J Nanomedicine. 2007; 2:191–9. [PubMed: 17722547]
45. Zhang C, Jugold M, Woenne EC, Lammers T, Morgenstern B, Mueller MM, et al. Specific targeting of tumor angiogenesis by RGD-conjugated ultrasmall superparamagnetic iron oxide particles using a clinical 1.5-T magnetic resonance scanner. Cancer Res. 2007; 67:1555–62. [PubMed: 17308094]
46. Lee HY, Li Z, Chen K, Hsu AR, Xu C, Xie J, et al. PET/MRI dual-modality tumor imaging using arginine-glycine-aspartic (RGD)-conjugated radiolabeled iron oxide nanoparticles. J Nucl Med. 2008; 49:1371–9. [PubMed: 18632815]
47. Chen K, Xie J, Xu H, Behera D, Michalski MH, Biswal S, et al. Triblock copolymer coated iron oxide nanoparticle conjugate for tumor integrin targeting. Biomaterials. 2009; 30:6912–9. [PubMed: 19773081]
48. Kang HW, Josephson L, Petrovsky A, Weissleder R, Bogdanov A Jr. Magnetic resonance imaging of inducible E-selectin expression in human endothelial cell culture. Bioconjug Chem. 2002; 13:122–7. [PubMed: 11792187]
49. Kang HW, Torres D, Wald L, Weissleder R, Bogdanov AA Jr. Targeted imaging of human endothelial-specific marker in a model of adoptive cell transfer. Lab Invest. 2006; 86:599–609. [PubMed: 16607378]
50. Reynolds PR, Larkman DJ, Haskard DO, Hajnal JV, Kennea NL, George AJ, et al. Detection of vascular expression of E-selectin in vivo with MR imaging. Radiology. 2006; 241:469–76. [PubMed: 17005768]
51. Boutry S, Laurent S, Elst LV, Muller RN. Specific E-selectin targeting with a superparamagnetic MRI contrast agent. Contrast Media Mol Imaging. 2006; 1:15–22. [PubMed: 17193596]
52. Yan C, Boyd DD. Regulation of matrix metalloproteinase gene expression. J Cell Physiol. 2007; 211:19–26. [PubMed: 17167774]
53. Lepage M, Dow WC, Melchior M, You Y, Fingleton B, Quarles CC, et al. Noninvasive detection of matrix metalloproteinase activity in vivo using a novel magnetic resonance imaging contrast agent with a solubility switch. Mol Imaging. 2007; 6:393–403. [PubMed: 18053410]
54. Olson ES, Jiang T, Aguilera TA, Nguyen QT, Ellies LG, Scadeng M, et al. Activatable cell penetrating peptides linked to nanoparticles as dual probes for in vivo fluorescence and MR imaging of proteases. Proc Natl Acad Sci U S A. 2010; 107:4311–6. [PubMed: 20160077]

NIH-PA Author Manuscript

NIH-PA Author Manuscript

NIH-PA Author Manuscript

55. Ye F, Wu X, Jeong EK, Jia Z, Yang T, Parker D, et al. A peptide targeted contrast agent specific to fibrin-fibronectin complexes for cancer molecular imaging with MRI. Bioconjug Chem. 2008; 19:2300–3. [PubMed: 19053180]
56. Tan M, Wu X, Jeong EK, Chen Q, Lu ZR. Peptide-Targeted Nanoglobular Gd-DOTA Monoamide Conjugates for Magnetic Resonance Cancer Molecular Imaging. Biomacromolecules. 2010; 11:754–61. [PubMed: 20131758]
57. Schellenberger EA, Bogdanov A Jr, Hogemann D, Tait J, Weissleder R, Josephson L. Annexin V-CLIO: a nanoparticle for detecting apoptosis by MRI. Mol Imaging. 2002; 1:102–7. [PubMed: 12920851]
58. Neves AA, Krishnan AS, Kettunen MI, Hu DE, Backer MM, Davletov B, et al. A paramagnetic nanoprobe to detect tumor cell death using magnetic resonance imaging. Nano Lett. 2007; 7:1419–23. [PubMed: 17411099]
59. Zhao M, Beauregard DA, Loizou L, Davletov B, Brindle KM. Non-invasive detection of apoptosis using magnetic resonance imaging and a targeted contrast agent. Nat Med. 2001; 7:1241–4. [PubMed: 11689890]
60. Jung HI, Kettunen MI, Davletov B, Brindle KM. Detection of apoptosis using the C2A domain of synaptotagmin I. Bioconjug Chem. 2004; 15:983–7. [PubMed: 15366950]
61. van Tilborg GA, Mulder WJ, Deckers N, Storm G, Reutelingsperger CP, Strijkers GJ, et al. Annexin A5-functionalized bimodal lipid-based contrast agents for the detection of apoptosis. Bioconjug Chem. 2006; 17:741–9. [PubMed: 16704213]
62. Reimer P, Weissleder R, Lee AS, Wittenberg J, Brady TJ. Receptor imaging: application to MR imaging of liver cancer. Radiology. 1990; 177:729–34. [PubMed: 2243978]
63. Weissleder R, Reimer P, Lee AS, Wittenberg J, Brady TJ. MR receptor imaging: ultrasmall iron oxide particles targeted to asialoglycoprotein receptors. AJR Am J Roentgenol. 1990; 155:1161–7. [PubMed: 2122660]
64. Towner RA, Smith N, Tesiram YA, Abbott A, Saunders D, Blindauer R, et al. In vivo detection of c-MET expression in a rat hepatocarcinogenesis model using molecularly targeted magnetic resonance imaging. Mol Imaging. 2007; 6:18–29. [PubMed: 17311762]
65. Reimer P, Weissleder R, Shen T, Knoefel WT, Brady TJ. Pancreatic receptors: initial feasibility studies with a targeted contrast agent for MR imaging. Radiology. 1994; 193:527–31. [PubMed: 7972773]
66. Shen TT, Bogdanov A Jr, Bogdanova A, Poss K, Brady TJ, Weissleder R. Magnetically labeled secretin retains receptor affinity to pancreas acinar cells. Bioconjug Chem. 1996; 7:311–6. [PubMed: 8816953]
67. Yang L, Mao H, Wang YA, Cao Z, Peng X, Wang X, et al. Single chain epidermal growth factor receptor antibody conjugated nanoparticles for in vivo tumor targeting and imaging. Small. 2009; 5:235–43. [PubMed: 19089838]
68. Montet X, Weissleder R, Josephson L. Imaging pancreatic cancer with a peptide-nanoparticle conjugate targeted to normal pancreas. Bioconjug Chem. 2006; 17:905–11. [PubMed: 16848396]
69. Fleischmann A, Laderach U, Friess H, Buechler MW, Reubi JC. Bombesin receptors in distinct tissue compartments of human pancreatic diseases. Lab Invest. 2000; 80:1807–17. [PubMed: 11140694]
70. Heckl S, Pipkorn R, Waldeck W, Spring H, Jenne J, von der Li C, et al. Intracellular visualization of prostate cancer using magnetic resonance imaging. Cancer Res. 2003; 63:4766–72. [PubMed: 12941791]
71. Konda SD, Aref M, Wang S, Brechbiel M, Wiener EC. Specific targeting of folate-dendrimer MRI contrast agents to the high affinity folate receptor expressed in ovarian tumor xenografts. MAGMA. 2001; 12:104–13. [PubMed: 11390265]
72. Kresse M, Wagner S, Pfefferer D, Lawaczeck R, Elste V, Semmler W. Targeting of ultrasmall superparamagnetic iron oxide (USPIO) particles to tumor cells in vivo by using transferrin receptor pathways. Magn Reson Med. 1998; 40:236–42. [PubMed: 9702705]
73. Hogemann-Savellano D, Bos E, Blondet C, Sato F, Abe T, Josephson L, et al. The transferrin receptor: a potential molecular imaging marker for human cancer. Neoplasia. 2003; 5:495–506. [PubMed: 14965443]

NIH-PA Author Manuscript

NIH-PA Author Manuscript

NIH-PA Author Manuscript

74. O'Donnell KA, Yu D, Zeller KI, Kim JW, Racke F, Thomas-Tikhonenko A, et al. Activation of transferrin receptor 1 by c-Myc enhances cellular proliferation and tumorigenesis. Mol Cell Biol. 2006; 26:2373–86. [PubMed: 16508012]
75. Artemov D, Mori N, Ravi R, Bhujwalla ZM. Magnetic resonance molecular imaging of the HER-2/neu receptor. Cancer Res. 2003; 63:2723–7. [PubMed: 12782573]
76. Slamon DJ, Clark GM, Wong SG, Levin WJ, Ullrich A, McGuire WL. Human breast cancer: correlation of relapse and survival with amplification of the HER-2/neu oncogene. Science. 1987; 235:177–82. [PubMed: 3798106]
77. Huh YM, Jun YW, Song HT, Kim S, Choi JS, Lee JH, et al. In vivo magnetic resonance detection of cancer by using multifunctional magnetic nanocrystals. J Am Chem Soc. 2005; 127:12387–91. [PubMed: 16131220]
78. Lee JH, Huh YM, Jun YW, Seo JW, Jang JT, Song HT, et al. Artificially engineered magnetic nanoparticles for ultra-sensitive molecular imaging. Nat Med. 2007; 13:95–9. [PubMed: 17187073]
79. Chen TJ, Cheng TH, Chen CY, Hsu SC, Cheng TL, Liu GC, et al. Targeted Herceptin-dextran iron oxide nanoparticles for noninvasive imaging of HER2/neu receptors using MRI. J Biol Inorg Chem. 2009; 14:253–60. [PubMed: 18975017]
80. Leuschner C, Kumar CS, Hansel W, Soboyejo W, Zhou J, Hormes J. LHRH-conjugated magnetic iron oxide nanoparticles for detection of breast cancer metastases. Breast Cancer Res Treat. 2006; 99:163–76. [PubMed: 16752077]
81. Yang L, Peng XH, Wang YA, Wang X, Cao Z, Ni C, et al. Receptor-targeted nanoparticles for in vivo imaging of breast cancer. Clin Cancer Res. 2009; 15:4722–32. [PubMed: 19584158]
82. Li X, Du X, Huo T, Liu X, Zhang S, Yuan F. Specific targeting of breast tumor by octreotide-conjugated ultrasmall superparamagnetic iron oxide particles using a clinical 3.0-Tesla magnetic resonance scanner. Acta Radiol. 2009; 50:583–94. [PubMed: 19449236]
83. Veiseh O, Sun C, Fang C, Bhattarai N, Gunn J, Kievit F, et al. Specific targeting of brain tumors with an optical/magnetic resonance imaging nanoprobe across the blood-brain barrier. Cancer Res. 2009; 69:6200–7. [PubMed: 19638572]
84. Bogdanov, A., Jr; DeLeo, M.; Shazeeb, M.; Kang, HW.; Sotak, C. Anti-EGF receptor antibody conjugates in MR imaging of human glioma xenografts using enzyme-mediated signal amplification [abstract]. Proc. 100th AACR Annual Meeting, (Meeting Abstracts); 2009. p. 3219
85. Bogdanov A Jr, DeLeo M, Shazeeb M, Kang HW, Sotak C. Paramagnetic substrate for molecular MR Imaging of EGF receptor in human glioma model using targeted antibody-conjugated enzymatic system [abstract]. Proc World Mol Imag Congr, (Meeting Abstracts). 2008:1781.
86. Bogdanov A, Querol Sans M, Kang HW, Bennett DG, Sotak C. EGF receptor expression imaging using antibody-conjugated enzymes and a paramagnetic substrate [abstract]. Proc Intl Soc Magn Reson Med (Meeting Abstracts). 2007:875.
87. Bogdanov A Jr, Kang HW, Querol M, Pretorius PH, Yudina A. Synthesis and testing of a binary catalytic system for imaging of signal amplification in vivo. Bioconjug Chem. 2007; 18:1123–30. [PubMed: 17508710]
88. Kufe DW. Mucins in cancer: function, prognosis and therapy. Nat Rev Cancer. 2009; 9:874–85. [PubMed: 19935676]
89. Moore A, Medarova Z, Potthast A, Dai G. In vivo targeting of underglycosylated MUC-1 tumor antigen using a multimodal imaging probe. Cancer Res. 2004; 64:1821–7. [PubMed: 14996745]
90. Medarova Z, Rashkovetsky L, Pantazopoulos P, Moore A. Multiparametric monitoring of tumor response to chemotherapy by noninvasive imaging. Cancer Res. 2009; 69:1182–9. [PubMed: 19141648]
91. Choi H, Choi SR, Zhou R, Kung HF, Chen IW. Iron oxide nanoparticles as magnetic resonance contrast agent for tumor imaging via folate receptor-targeted delivery. Acad Radiol. 2004; 11:996–1004. [PubMed: 15350580]
92. Weissleder R, Kelly K, Sun EY, Shtatland T, Josephson L. Cell-specific targeting of nanoparticles by multivalent attachment of small molecules. Nat Biotechnol. 2005; 23:1418–23. [PubMed: 16244656]

NIH-PA Author Manuscript

NIH-PA Author Manuscript

NIH-PA Author Manuscript

93. Lee JH, Huh YM, Jun YW, Seo JW, Jang JT, Song HT, et al. Artificially engineered magnetic nanoparticles for ultra-sensitive molecular imaging. Nat Med. 2007; 13:95–9. [PubMed: 17187073]

94. Lee JH, Sherlock SP, Terashima M, Kosuge H, Suzuki Y, Goodwin A, et al. High-contrast in vivo visualization of microvessels using novel FeCo/GC magnetic nanocrystals. Magn Reson Med. 2009; 62:1497–509. [PubMed: 19859938]

95. Das M, Mishra D, Dhak P, Gupta S, Maiti TK, Basak A, et al. Biofunctionalized, phosphonate-grafted, ultrasmall iron oxide nanoparticles for combined targeted cancer therapy and multimodal imaging. Small. 2009; 5:2883–93. [PubMed: 19856326]

96. Jain TK, Richey J, Strand M, Leslie-Pelecky DL, Flask CA, Labhasetwar V. Magnetic nanoparticles with dual functional properties: drug delivery and magnetic resonance imaging. Biomaterials. 2008; 29:4012–21. [PubMed: 18649936]

97. Rahimi, M.; Wadajkar, A.; Subramanian, K.; Yousef, M.; Cui, W.; Hsieh, JT., et al. In vitro evaluation of novel polymer-coated magnetic nanoparticles for controlled drug delivery. Nanomedicine. Epub 2010 Feb 18, Available from www.sciencedirect.com/science/journal/15499634

98. Aime S, Castelli DD, Crich SG, Gianolio E, Terreno E. Pushing the sensitivity envelope of lanthanide-based magnetic resonance imaging (MRI) contrast agents for molecular imaging applications. Acc Chem Res. 2009; 42:822–31. [PubMed: 19534516]

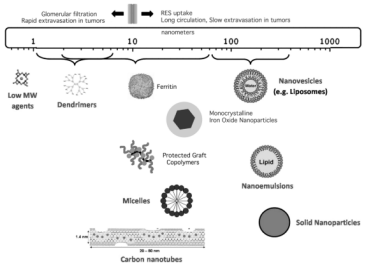

Figure 1.
Average size of the nanocarriers considered so far for developing highly sensitive Gd(III)-based MRI agents. Adapted from [97].

NIH-PA Author Manuscript
NIH-PA Author Manuscript
NIH-PA Author Manuscript

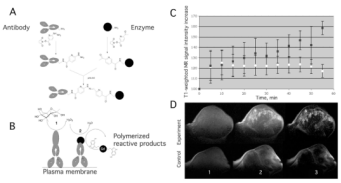

Figure 2.

A) Schema of mAb conjugate synthesis with a formation of stable bisatomatic hydrazone bond using HydraLinK. B) HRP/GO-targeted coupled catalysis in the presence of glucose. Di-5HT-DTPA(Gd) is used as a reducer of oxidized HRP. Top: Plot of signal intensity (SI) vs. time within tumor ROI. (Squares – treated; circles – control). Data shown as mean±SD (n=4). Bottom: Representative 2.0T MRIs of mouse A431 tumor xenograft pre- and post-injection of 5HT-DTPAGd substrate. MRIs in upper row from animal pre-injected with L6 mAb conjugates. Lower row shows control tumor MRIs. Pre- (A, scan 1), post- (B, scan 12), and subtraction (C, scan 12 – scan 1). [37].

NIH-PA Author Manuscript NIH-PA Author Manuscript NIH-PA Author Manuscript

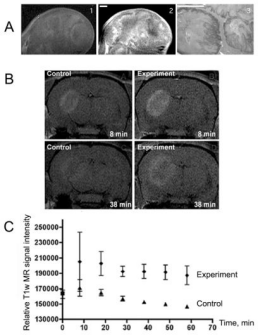

Figure 3.

A) MRamp imaging of EGF receptor expression in A431 squamous carcinoma tumor xenograft: **1**- T1w SE image of A431 xenograft obtained after the injection of: A- 0.2 mmol/kg di-5-HT-DTPA(Gd) alone; **2**- after the sequential injection of 20 μg of EGFR mAb conjugates followed by di-5-HT-DTPA(Gd). **3**- anti-EGFR staining of tumor section. (Bars=1 mm). **B)** Representative T1w SE (TR/TE=700/15) images of EGFR-expressing human Gli36 glioma tumors after the injection of di-tyramide of GdDTPA in the absence or in the presence of preinjected anti-EGFR mAb-GO and mAb-HRP conjugates. **C**- Time course of the corresponding MR SI change (mean±95%CI are shown, n=3). [36].

NIH-PA Author Manuscript NIH-PA Author Manuscript NIH-PA Author Manuscript

NIH-PA Author Manuscript

NIH-PA Author Manuscript

NIH-PA Author Manuscript

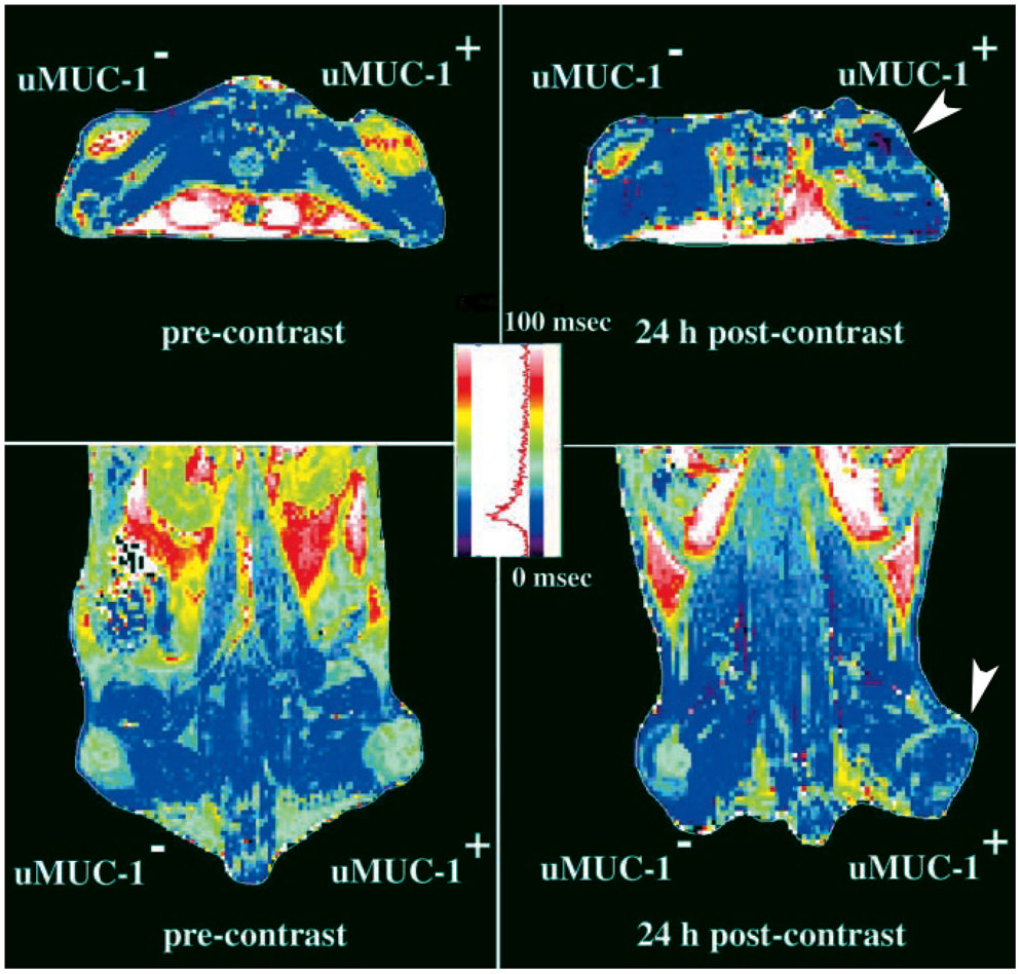

Figure 4.

Representative colorized T2 maps of the animals bearing underglycosylated mucin-1 antigen (uMUC-1)-negative (U87) and uMUC-1-positive (LS174T) contralateral tumors (shown by an arrowhead). Transverse (*top*) and coronal (*bottom*) images showed a significant decrease in signal intensity in uMUC-1-positive tumors 24 h after administration of the CLIO-EPPT probe. Reprinted with permission from [88].